Journal of Materials Chemistry A

Physicochemical implications of alkoxide "mixing" in polyoxovanadium clusters for nonaqueous energy storage

Journal:	*Journal of Materials Chemistry A*
Manuscript ID	TA-ART-12-2018-012306.R1
Article Type:	Paper
Date Submitted by the Author:	24-Jan-2019
Complete List of Authors:	VanGelder, Lauren; University of Rochester, Department of Chemistry Schreiber, Eric; University of Rochester, Department of Chemistry Matson, Ellen; University of Rochester, Chemistry

Journal of Materials Chemistry A

ARTICLE

Physicochemical implications of alkoxide "mixing" in polyoxovanadium clusters for nonaqueous energy storage

Lauren E. VanGelder,[a] Eric Schreiber, [a] and Ellen M. Matson *[a]

Received 00th January 20xx,
Accepted 00th January 20xx

DOI: 10.1039/x0xx00000x

www.rsc.org/

Identification of suitable charge carriers is essential for the success of nonaqueous energy storage systems. Thus, elucidation of structural parameters which affect the physicochemical properties of a molecule in organic solvent is of critical importance. Here, we continue our work related to the development of polyoxovanadium-alkoxide clusters for nonaqueous energy storage through the synthesis and subsequent analysis of a series of "mixed"-alkoxide clusters, $[V_6O_7(OR)_{12-x}(OCH_3)_x]$ (R = C_2H_5, C_3H_7, C_4H_9, C_5H_{11}, C_6H_{13}). We determine that the presence of a mixture of bridging-alkoxides enhances both the physical and electrochemical behaviour of the clusters in nonaqueous energy storage schematics, evidenced by increased solubility and electron-transfer kinetics. These results provide insight into the consequences of using a classically "impure" system, revealing how synergistic behaviour of a mixture of compounds can yield improved function over that of a pure solution.

Introduction

Grid-scale energy storage devices are critical for improving the efficiency of our current electrical grid and enabling the smooth integration of stochastic renewables.[1-3] To date, however, the application of such devices has been limited, owing to the lack of an efficient and economically viable technology.[4, 5] As such, research into the development of stationary energy storage is experiencing a massive surge, with a wide array of innovations and inventions appearing in recent years.[6, 7] Among those receiving the most attention are redox flow batteries (RFBs), which use charge-storing redox-active species in liquid electrolytes to interconvert electrical and chemical energy.[8-10] The unique design of this technology is the source of its appeal, as it enables decoupled power and energy scaling, while promising long lifetimes, facile maintenance, and simplified manufacturing over other battery technologies.[11] Despite these attractive features, adoption of RFBs remains limited by the high cost of device production.[12]

In order to increase the viability of RFB technology, researchers have focused on the development of efficient charge carriers, with a host of inorganic, organic, and polymer-based materials reported for this application.[13-22] Although the majority of reported electrolytes are designed for use in aqueous media, there is a growing interest in the development of charge carriers that are compatible with nonaqueous solvents.[13, 23] This is principally due to the fact that the use of organic solvent as a flow medium could enable larger cell potentials and faster charging/discharging than aqueous systems.[13, 23-25] In addition, use of nonaqueous solvents broadens the range of applicable molecules, potentially creating pathways to lower overall costs of RFB systems.[26] Of particular importance to the synthetic design of new charge carriers for nonaqueous redox flow battery (NRFB) application is the development of a comprehensive understanding of structural parameters that influence the relevant physicochemical properties; namely: the stability, solubility, volumetric potential, diffusion, and electron-transfer kinetics of the redox-active species in solution.[12, 23] Such insights have been leveraged to great effect in both organic[21, 27] and metal-based[28-30] charge carriers for nonaqueous energy storage, highlighting the importance of fundamental investigations into the structure-function relationships that dictate molecular capabilities.

[a]*Department of Chemistry, University of Rochester, Rochester, New York 14627*
E-mail: matson@chem.rochester.edu

Electronic Supplementary Information (ESI) available: See DOI: 10.1039/x0xx00000x

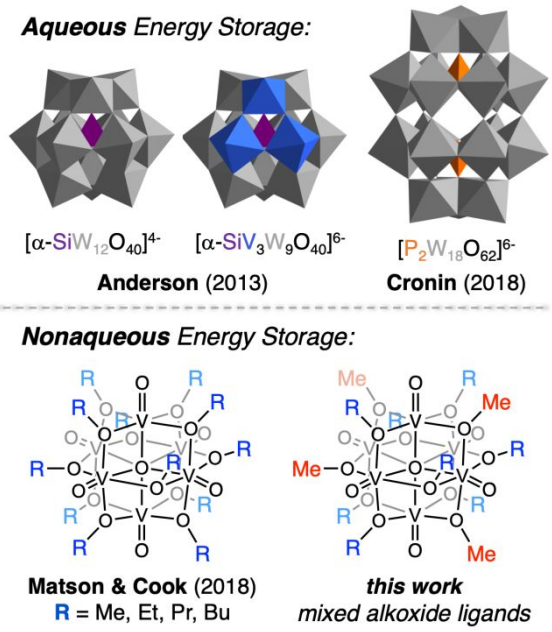

Figure 1. Polyoxometalate clusters previously reported for applications in flow electrochemical energy storage.[40, 42,45, 50]

Polyoxometalates (POMs), a family of molecular metal-oxides consisting of three or more transition metal oxyanions, are rapidly gaining interest for application in energy storage.[31-34] This is principally due to the fact that these discreet polynuclear metal-oxide assemblies are typically generated through self-assembly pathways, possess a high degree of tunability (size, shape, surface functionalization, metal composition, etc.), and exhibit bench-top stabilities and rich redox profiles.[35-38] Although collectively the aforementioned markers suggest that POMs would be ideal for RFB applications, there are few investigations into the solution-state energy storage capabilities of these systems (Figure 1). Anderson and coworkers first reported the application of POMs for RFBs, describing the use of a series of mixed-metal Keggin-type clusters in aqueous charging schematics.[39-41] More recently, Cronin and coworkers reported a water soluble $[P_2W_{18}O_{62}]^{6-}$ core that can accommodate eighteen electrons and protons per anion.[42] Likewise, Stimming and coworkers demonstrate the use of two different POMs, $[SiW_{12}O_{40}]^{4-}$ and $[PV_{14}O_{42}]^{9-}$, to generate an asymmetric aqueous RFB capable of rapid multi-electron transfer.[43] Yet the application of POMs for *nonaqueous* energy storage remains limited, owing to low solubility and poor stability of these assemblies in organic solvent.[39, 44]

Over the past year, we have established a unique family of POMs, the polyoxovanadium-alkoxide (POV-alkoxide) clusters, as effective charge carriers for NRFB application (Figure 1).[45-47] The incorporation of twelve bridging-alkoxide ligands to flank the hexavanadate cluster core yields a neutral, mixed-valent ($V^V_2V^{IV}_4$) system $[V_6O_7(OR)_{12}]$. This alkoxide-bridged structure affords measurable solubility in acetonitrile and an electrochemical profile containing four reversible redox events over a two-volt window. Furthermore, this platform is uniquely modular, able to be synthesized with a range of bridging alkoxide ligands (OR^-, R = CH_3, C_2H_5, C_3H_7, and C_4H_9) and multidentate functionalities (TRIOL).[47-49] We have demonstrated that while the identity of the bridging alkoxide ligands has significant bearing on both the solubility and the electrochemical stability of the clusters, the electron-transfer rate constants and diffusion kinetics remain consistently rapid. The combined physical and electrochemical properties of this distinct class of organo-functionalized polyoxovanadate clusters makes them promising candidates for nonaqueous energy storage application.

Here, we continue our efforts toward understanding the influence of bridging-alkoxide identity on the functionality of POV-alkoxide-based charge carriers. We report the formation of two new long-chain homoleptic alkyl compounds, $[V_6O_7(OR)_{12}]$ (R = C_5H_{11}, C_6H_{13}), establishing the limits in alkyl chain length with respect to the transport and redox chemistry of these systems. We also introduce five "mixed" alkoxide clusters, $[V_6O_7(OR)_{12-x}(OCH_3)_x]$ (R = C_2H_5, C_3H_7, C_4H_9, C_5H_{11}, C_6H_{13}), where the value of "x" is variable within a single product. Interestingly, despite their composition being technically "impure" (i.e. a *mixture* of compounds), these POV-alkoxides demonstrate the same four distinct redox events exhibited by the homoleptic compounds. Furthermore, the mixed-alkoxide clusters possess improved solubilities and enhanced electrochemical stability over their respective homoleptic congeners, yielding a more energy-dense charge carrier for NRFB application. These studies tap into the idea of synergistic reactivity—a common theme across medicinal chemistry and materials science—and provide insight into the implication of introducing "defects" at the surface of polynuclear charge carriers for the purpose of improved function for stationary energy storage.

Results & Discussion

Synthesis of homoleptic POV-alkoxides $[V_6O_7(OR)_{12}]$ (1)

In our first report describing the application of POV-alkoxide clusters for nonaqueous energy storage, we reported that the methoxide-bridged cluster $[V_6O_7(OCH_3)_{12}]$ (**1-methyl**) is prone to decomposition at potentials ≥ 1 V.[45] Fortunately, the oxidative instability of this cluster could be resolved by substitution of the twelve bridging-methoxides for longer alkoxide moieties. Indeed, evaluation of the electrochemical properties of $[V_6O_7(OC_2H_5)_{12}]$ (**1-ethyl**), $[V_6O_7(OC_3H_7)_{12}]$ (**1-propyl**) and $[V_6O_7(OC_4H_9)_{12}]$ (**1-butyl**) revealed improved redox stability of the clusters across *all five* charge states suggested by CV.[45, 50] Interestingly, despite the increase in alkyl chain length, the redox profiles, diffusion coefficients, and heterogeneous electron-transfer rates all remained relatively consistent for **1-methyl**, **1-ethyl**, **1-propyl**, and **1-butyl**.[50] The solubility of these systems, on the other hand, showed significant variability, ranging from 0.05 M for **1-ethyl** to 0.30 M for **1-butyl**. Collectively, these results suggest that further modification of the surface ligands may improve the physical properties of POV-alkoxides, without perturbing their electrochemical characteristics.

To understand the extent to which alkyl chain length can be tolerated by the POV-alkoxide framework, we targeted the synthesis of two longer-chain alkoxide clusters, $[V_6O_7(OC_5H_{11})_{12}]$ (**1-pentyl**) and $[V_6O_7(OC_6H_{13})_{12}]$ (**1-hexyl**). For the shorter-chain POV-alkoxide clusters (e.g. **1-methyl**, **1-ethyl**, **1-propyl**, **1-butyl**), the established syntheses of the Lindqvist core calls for the use of a vanadium(V) oxytris-alkoxide precursor, $VO(OR)_3$, where R is the desired bridging alkoxide in the final cluster,

Scheme 1. Synthesis of homoleptic clusters **1-pentyl** and **1-hexyl**.

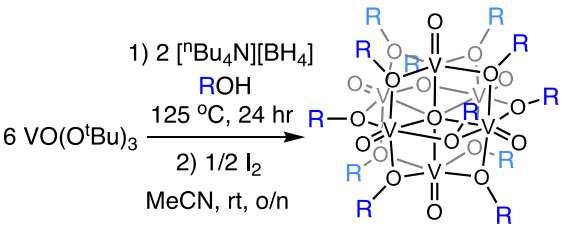

$[V_6O_7(OR)_{12}]$ (R = CH_3, C_2H_5, C_3H_7, C_4H_9). However, generation and isolation of the analogous vanadium(V) oxytris-pentoxide and -hexaoxide precursors proved challenging. Instead, we attempted cluster synthesis using a vanadium(V) oxytris-tertbutoxide precursor, $VO(O^tBu)_3$. Indeed, the solvothermal reaction of $VO(O^tBu)_3$ with two equivalents of an external reductant, tetrabutylammonium borohydride ($[^nBu_4N][BH_4]$, in the appropriate solvent, R-OH, (R = C_5H_{11} or C_6H_{13} for **1-pentyl** and **1-hexyl**, respectively) afforded the mono-anionic form of each long-chain POV-alkoxide, $[^nBu_4N][V_6O_7(OR)_{12}]$. To isolate the neutral cluster, the reduced scaffolds were stirred overnight with half an equivalent of I_2, mirroring established procedures for mild oxidation of anionic POV-alkoxides.[47-49, 51] Under these reaction conditions, complexes **1-pentyl** and **1-hexyl** can be obtained in good yield (87 % and 70 %, respectively, Scheme 1). Formation of the desired clusters was confirmed by ^{1}H NMR, electrospray ionization mass spectrometry (ESI-MS), and IR spectroscopy (Figures S1-S3).

Unlike their shorter-chain counterparts, the long-chain POV-alkoxides **1-pentyl** and **1-hexyl** are both liquids at room temperature. Although our hope was that these compounds would possess significant solubility in acetonitrile, thereby improving energy density in NRFB application, we found that both **1-pentyl** and **1-hexyl** demonstrated fairly significant immiscibility with acetonitrile, limiting their overall "solubility". This effect is more pronounced with increasing alkyl-chain length, yielding overall solubilities of 0.10 M (**1-pentyl**) and 0.06 M (**1-hexyl**) (Table 1, Figures S4-S5).

To examine the redox properties of **1-pentyl** and **1-hexyl**, cyclic voltammograms (CV) for each complex were measured in acetonitrile. Electrochemical analysis of **1-pentyl** reveals, as expected, four quasi-reversible redox events, consistent with the previous homoleptic POV-alkoxide clusters **(1-methyl**, **1-ethyl**, **1-propyl**, **1-butyl**; Table 1, Figure 2**).** Each one-electron redox event can be assigned to the formal oxidation of a single vanadyl ion ($V^{IV} \rightarrow V^{V}$) of the Lindqvist core.[48,51,52] However given the delocalization of electron density in the POV-alkoxide assembly, it is likely that these changes in charge state are evenly distributed across all six vanadyl ions of the cluster core.[48,54] While no significant trends are observed in the slight shifts in $E_{1/2}$ values of the four vanadium-based redox events, we do note that the "outer" redox events ($E_{1/2}$ = −0.96 & 0.85 V) have ratios of cathodic to anodic peak current (i_c/i_a) which deviate from unity. This is in contrast to the i_c/i_a ratios for the "inner" two redox events ($E_{1/2}$ = −0.36 & 0.25 V) which approach a value of 1.00, consistent with reversible electron transfer. This result is distinct for complex **1-pentyl**, as the 1-electron redox events for the shorter-chain POV-alkoxide clusters are internally consistent within the series, indicating that all electron transfer events are reversible electrochemical processes.

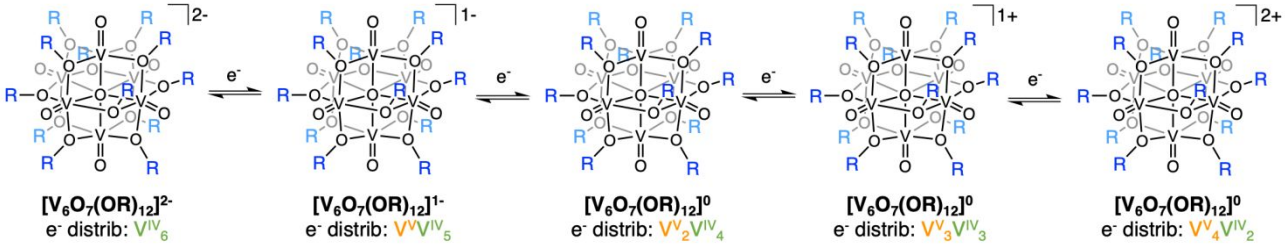

Scheme 2. Changes in oxidation state distribution of vanadyl ions across the four observed redox events of mixed-valent POV-alkoxide clusters.

Table 1. Solubility and electrochemical parameters of all complexes.

Complex	Solubility (M)	V^{IV}_6 / $V^{V}_1V^{IV}_5$ couple[a]	$V^{V}_1V^{IV}_5$ / $V^{V}_2V^{IV}_4$ couple[a]	$V^{V}_2V^{IV}_4$ / $V^{V}_3V^{IV}_3$ couple[a]	$V^{V}_3V^{IV}_3$ / $V^{V}_4V^{IV}_2$ couple[a]
1-Methyl	0.202	−0.72 (0.99)	−0.22 (1.01)	0.30 (1.00)	0.85 (1.02)
1-Ethyl	0.048	−0.88 (0.98)	−0.34 (1.00)	0.22 (1.00)	0.79 (1.01)
1-Propyl	0.097	−0.89 (0.98)	−0.33 (0.99)	0.25 (1.02)	0.83 (1.03)
1-Butyl	0.297	−0.94 (0.96)	−0.35 (0.99)	0.24 (1.00)	0.83 (1.03)
1-Pentyl	0.101	−0.96 (0.89)	−0.36 (0.98)	0.25 (1.06)	0.85 (1.07)
1-Hexyl	0.055	−1.50 (0.00)	−0.32 0.37)	0.30 (3.13)	1.11 (27.7)
2-Ethyl	0.071	−0.85 (1.05)	−0.32 (1.04)	0.24 (1.01)	0.81 (1.03)
2-Propyl	0.174	−0.83 (0.89)	−0.30 (1.05)	0.27 (1.01)	0.83 (1.01)
2-Butyl	0.399	−0.84 (0.95)	−0.29 (0.99)	0.28 (1.03)	0.83 (1.04)
2-Pentyl	0.267	−0.84 (0.92)	−0.29 (1.04)	0.27 (1.06)	0.84 (1.08)
2-Hexyl	0.131	−0.79 (0.75)	−0.28 (0.91)	0.28 (1.08)	0.93 (1.30)

[a] Standard potentials (measured *vs.* Ag/Ag^+) identified using cyclic voltammetry at 100 mV s^{-1} of 1 mM solutions of each complex with 0.1 M $[^nBu_4N][PF_6]$ supporting electrolyte in acetonitrile. Values in parentheses indicate ratios of the cathodic to anodic peak heights (i_c/i_a).

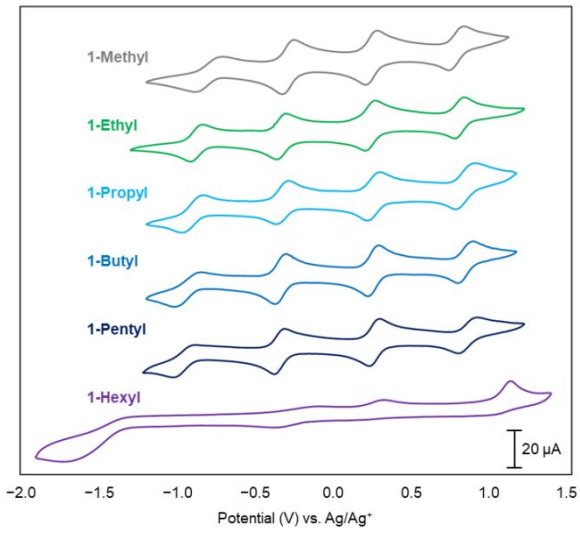

Figure 2. Cyclic voltammograms of homoleptic POV-alkoxides at 1 mM concentration measured in acetonitrile with 0.1 M $[^nBu_4N][PF_6]$ supporting electrolyte. Scan rate 100 mV/s, open circuit potential ~0 V for all species.

In contrast, the CV of **1-hexyl** deviates significantly from all other POV-alkoxide clusters reported to date (Figure 2). Although four redox events can be made out in the CV of complex **1-hexyl** (See supporting information for detail, Figure S6), the $E_{1/2}$ values differ significantly from the previously discussed systems, and the reversibility of all events is diminished, as reflected in the i_c/i_a ratios (Table 1). Given the poor compatibility (low miscibility) of the long-chained alkoxide cluster (**1-hexyl**) with acetonitrile, we repeated CV experiments in a less polar solvent, dichloromethane (DCM). Despite complete miscibility of **1-hexyl** in DCM, we found that the CV shows a similar electrochemical trace to that collected in acetonitrile (Figure S7). Thus, we can conclude that the poor reversibility of redox events is not a result of cluster incompatibility with the solvent, but instead is likely a result of decreased diffusion rates due to the increased size of the Lindqvist core of **1-hexyl**. This important result captures a molecular limit to ligand modification, revealing crucial design criteria for engineering POV-alkoxide clusters for energy storage.

Synthesis of mixed POV-alkoxides $[V_6O_7(OR)_{12-x}(OCH_3)_x]$ (2)

In examining the trends in solubility for the homoleptic POV-alkoxide series $[V_6O_7(OR)_{12}]$ (**1**), we note that complex **1-butyl** possesses the highest solubility in acetonitrile (Table 1). Interestingly, this is the only cluster that also exhibits an "impurity" the persists following purification, where approximately 30 % of the molecules contain a single bridging-butoxide ligand replaced with a methoxide moiety ($[V_6O_7(OC_4H_9)_{11}(OCH_3)]$).[50] This molecular impurity, though clearly detectable by ESI-MS (Figure S8), is not observed in the ^{1}H NMR spectrum of **1-butyl**.[50] Likewise, the CV of complex **1-butyl** bears four, well-defined electrochemical events, despite formally being a mixture of two species (Figure 2). The lack of a detectable byproduct by CV is striking, as in the mixture of $[V_6O_7(OCH_3)_{12}]$ and $[V_6O_8(OCH_3)_{11}]$, where a single methoxide ligand is substituted for a bridging oxide moiety, a distinct set of reversible waves can be observed.[48, 52] The uniform CV of **1-butyl** suggests that the solution-state electrochemical behaviour of the mixture is comparable to what would be expected from a "pure" solution. Furthermore, we hypothesized that it is the presence of this "impurity" that improves the solubility of **1-butyl** in acetonitrile, as the overall symmetry of the mixed-ligand species, $[V_6O_7(OC_4H_9)_{11}(OCH_3)]$, is reduced, thereby disfavouring solid-state crystal packing of the molecule.[47, 53] These striking results prompt the following questions for continued investigation: 1) Would further reduction in symmetry *via* substitution of bridging alkoxide ligands increase solubility? And 2) Would additional ligand substitutions influence the electrochemical behaviour of the hexavanadate core? Interested in better understanding the physicochemical properties of these mixtures, we set out to develop synthetic procedures to deliberately access a series of heteroleptic ("impure") POV-alkoxide clusters.

Toward the synthesis of a series of heteroleptic organo-functionalized polyoxovanandates, we sought to develop self-assembly protocols for a series of POV-alkoxide clusters bearing mixtures of bridging methoxide ligands and the corresponding higher order alkoxide (e.g. ethoxide, propoxide, butoxide, pentoxide, hexaoxide). We hypothesized that by using the $VO(OCH_3)_3$ precursor in place of the vanadyl alkoxyester we could generate a solvothermal reaction where the methoxide

Scheme 3. Synthesis of heteroleptic POV-alkoxides. All reactions yield a mixture of products, varying in the number of bridging alkoxide ligands substituted by methoxide moieties. See text and supporting information for details on distribution of products formed.

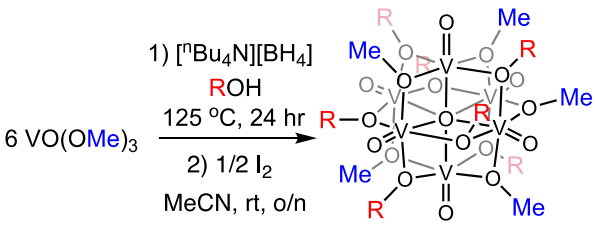

ligands can compete for coordination sites with the kinetically accessible alcohol (Scheme 3).

For example, to generate a mixed methoxide/ethoxide cluster, we reacted $VO(OCH_3)_3$, with *ethanol* and the external reductant $[^nBu_4N][BH_4]$ (Scheme 3). Following heating to 125 °C for 24 h, a green solution resulted, which was then reacted with half an equivalent of I_2 overnight to obtain a neutral product. Analysis of this compound by ESI-MS revealed an interesting distribution of products. Rather than m/z = 790, which would be observed for **1-methyl**, or m/z = 958, which corresponds to the anticipated molecular weight of **1-ethyl**, the ESI-MS of the crude product possesses a series of peaks (m/z = 944 $[V_6O_7(OC_2H_5)_{11}(OCH_3)]$); 930 ($[V_6O_7(OC_2H_5)_{10}(OCH_3)_2]$); 916 ($[V_6O_7(OC_2H_5)_9(OCH_3)_3]$); 902 ($[V_6O_7(OC_2H_5)_8(OCH_3)_4]$); 888 ($[V_6O_7(OC_2H_5)_7(OCH_3)_5]$); and 874 ($[V_6O_7(OC_2H_5)_6(OCH_3)_6]$) dispersed in a normal distribution (Figure 3). This reaction was

repeated in triplicate, each time affording an identical product distribution as confirmed by ESI-MS, indicating that the extent of methyl substitution by ethoxide ligands is consistent and reproducible (Figure S9). As such, we refer to this "mixed" product as $[V_6O_7(OC_2H_5)_{12-x}(OCH_3)_x]$ (**2-ethyl**), where "x" varies from 1 – 6 per the distribution of molecular weights observed by ESI-MS.

In order to test the generalizability of the formation of mixed POV-alkoxides, we reacted the methoxide starting material, $VO(OCH_3)_3$, under identical solvothermal synthetic protocols with primary alcohols ranging in chain length from 3-6 carbons. Similar to the results with ethanol, we found that the use of longer-chain alcohols gave rise to normal distributions of products with molecular masses corresponding to the species $[V_6O_7(OR)_{12-x}(OCH_3)_x]$. In the case of propanol, the product distribution was such that x = 1 – 6 for $[V_6O_7(OC_3H_7)_{12-x}(OCH_3)_x]$ (**2-propyl**, Figure S10). In analogous fashion, reaction in butanol yields a product distribution for $[V_6O_7(OC_4H_9)_{12-x}(OCH_3)_x]$ (**2-butyl**), with x = 1 – 7; in pentanol, a product distribution for $[V_6O_7(OC_5H_{11})_{12-x}(OCH_3)_x]$ (**2-pentyl**), with x = 3 – 8; and in hexanol, a distribution for $[V_6O_7(OC_6H_{13})_{12-x}(OCH_3)_x]$ (**2-hexyl**), with x = 3 – 9 (Figure S10).

Although the synthetic procedures are identical for each of the respective mixed POV-alkoxides, we note that the average number of incorporated methoxide-bridges varies systematically across the series. This variation seems to depend on the number of carbons of the remaining alkoxide ligands, with longer-chain alkoxides resulting in a higher degree of methoxide substitution, per mixture. For example, in the case of **2-ethyl**, the value of x ranges from 1 – 6, with the distribution of masses centred on the cluster where three bridging ethoxide ligands have been replaced by methoxide moieties (x = 3). In the case of **2-propyl**, this distribution observed in the ESI-MS lies between x = 3 & 4; for **2-butyl**, on x = 4; for **2-pentyl**, on x = 5; and for **2-hexyl** on x = 6 (Figure S11). We associate this trend with the increased sterics at the POV-alkoxide core during cluster self-assembly in the case of larger alcohols, necessitating retention of a higher percentage of methoxide ligands. However, this phenomenon could also be a result of the increased nucleophilicity of methoxide ligands over their longer alkyl-chain alcohol counter-parts.

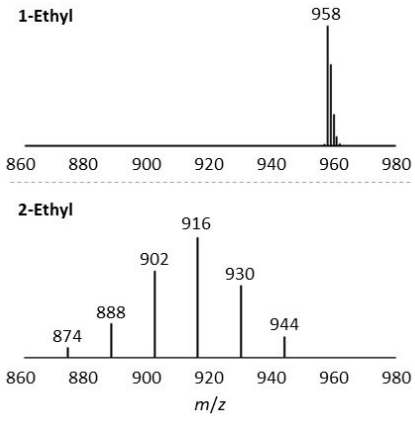

Figure 3. ESI-MS of homoleptic **1-ethyl** and mixed **2-ethyl** measured in acetonitrile. Full spectra in Figure S9.

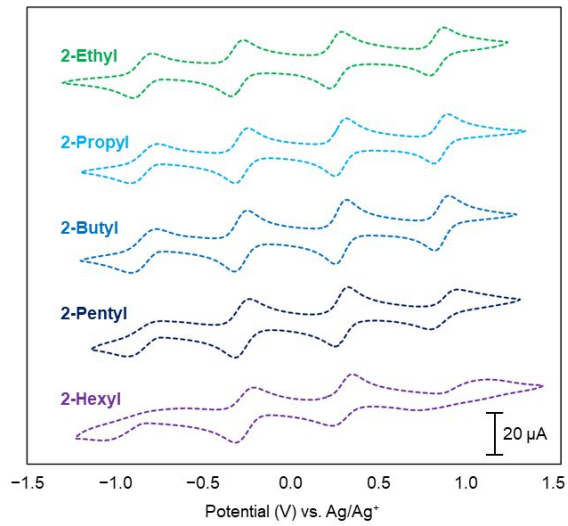

Figure 4. Cyclic voltammograms of mixed POV-alkoxides at 1 mM concentration measured in acetonitrile with 0.1 M $[^nBu_4N][PF_6]$ supporting electrolyte. Scan rate 100 mV/s, open circuit potential ~0 V for all species.

In addition to ESI-MS, characterization of the mixed POV-alkoxide clusters was performed using ^{1}H NMR, IR, and electronic absorbance spectroscopies. As with the ^{1}H NMR of each homoleptic cluster, each of the mixed POV-alkoxides exhibits a single broad paramagnetic resonance, centred around ~21 ppm (Figure S12). The remainder of the spectrum is featureless, suggesting no ^{1}H NMR-active impurities in these samples. The IR spectra of each complex increases in complexity with increasing alkyl chain length (**2-ethyl**–**2-hexyl**), yet bands corresponding to O—R bending and V=O_t stretching modes are clearly observed in the fingerprint region (Figure S13). Electronic absorption spectroscopy reveals two transitions for each compound, located at ~400 and ~1000 nm. Such features have been assigned to intervalence charge-transfer (IVCT) events in mixed-valent POV-alkoxides.[45, 54] The IR and electronic absorption data suggests, in all cases, that the non-symmetric substitution of alkoxide ligands does not disrupt the delocalization of electron density across the Lindqvist core.

Electrochemical analysis of each of the "mixed" POV-alkoxide clusters by CV reveals four redox events spanning ~2 V, closely resembling the redox profiles of the homoleptic derivatives (Figure 4, Table 1). For the mixed-alkoxide clusters from **1-ethyl** to **1-pentyl**, both the $E_{1/2}$ values and i_c/i_a ratios appear largely unchanged for each of the four redox events. However, in the case of the POV-hexaoxide cluster, it is clear that the species containing bridging methoxide moieties (**2-hexyl**) has significantly improved electrochemical properties over its homoleptic analogue, **1-hexyl** (Figure S14 & S15). The $E_{1/2}$ values and i_c/i_a ratios for the four redox events in **2-hexyl** are consistent with those expected for POV-alkoxide clusters. This result suggests that substitution of some of the bridging-hexaoxide ligands for bridging-methoxide moieties yields improved redox properties in acetonitrile. Based on this effect

Table 2. Diffusion coefficients for each neutral species, and heterogeneous electron transfer rate constants for each redox event of each complex. Values for **1-Methyl**, **1-Ethyl**, **1-Propyl**, and **1-Butyl** from previous work.[50]

		$V^{IV}_6/V^{IV}_5V^{V}_1$ couple	$V^{IV}_5V^{V}_1/V^{IV}_4V^{V}_2$ couple	$V^{IV}_4V^{V}_2/V^{I}_3V^{V}_3$ couple	$V^{IV}_3V^{V}_3/V^{IV}_4V^{V}_2$ couple
Complex	D_0 (cm^2 s^{-1})	k_0 (cm s^{-1})	k_0 (cm s^{-1})	k_0 (cm s^{-1})	k_0 (cm s^{-1})
1-Methyl	1.40 x 10^{-6}	1.70 x 10^{-2}	9.30 x 10^{-3}	1.40 x 10^{-2}	2.00 x 10^{-2}
1-Ethyl	5.44 x 10^{-6}	1.33 x 10^{-2}	8.46 x 10^{-3}	2.09 x 10^{-1}	1.25 x 10^{-1}
1-Propyl	5.20 x 10^{-6}	5.60 x 10^{-3}	2.10 x 10^{-2}	6.80 x 10^{-2}	2.50 x 10^{-2}
1-Butyl	2.22 x 10^{-5}	2.48 x 10^{-3}	1.37 x 10^{-2}	6.95 x 10^{-2}	5.20 x 10^{-2}
1-Pentyl	1.76 x 10^{-6}	9.98 x 10^{-3}	1.76 x 10^{-2}	3.63 x 10^{-2}	1.62 x 10^{-3}
1-Hexyl	--	--	--	--	--
2-Ethyl	2.09 x 10^{-6}	5.42 x 10^{-3}	3.01 x 10^{-2}	4.04 x 10^{-2}	5.80 x 10^{-3}
2-Propyl	2.45 x 10^{-5}	5.37 x 10^{-3}	3.64 x 10^{-1}	2.18 x 10^{-1}	9.53 x 10^{-3}
2-Butyl	3.32 x 10^{-5}	4.68 x 10^{-3}	1.49 x 10^{-1}	3.80 x 10^{-1}	9.42 x 10^{-3}
2-Pentyl	2.60 x 10^{-5}	3.93 x 10^{-3}	3.20 x 10^{-2}	5.58 x 10^{-2}	1.00 x 10^{-2}
2-Hexyl	1.35 x 10^{-6}	--	8.35 x 10^{-3}	8.35 x 10^{-3}	2.72 x 10^{-3}

being most pronounced in the POV-hexaoxide clusters, we hypothesize that the improved electrochemical properties of the mixed systems are a result of the smaller overall size of the molecule, which improves the diffusion of the molecule in solution.

The solubilities for each of the mixed POV-alkoxides were measured using analogous methods to those described for **1-pentyl** and **1-hexyl** (Figures S16-S20). For each of the heteroleptic clusters, solubility is improved over their corresponding homoleptic congener (Figure 5, Table 1). In fact, we note that the aforementioned improvements to the solubility of the mixed POV-alkoxides become even more pronounced as alkyl chain length increases.

Electrochemical analysis of POV-alkoxides

To more rigorously assess the electrochemical properties of the newly synthesized POV-alkoxides, heterogeneous electron-transfer rates and diffusion coefficients were calculated for each cluster. Using peak current values (i_p) obtained from CV data measured at scan rates from 100 – 1500 mV/s, the Randles-Sevcik relationship was used to determine the diffusion coefficients for each neutral cluster (Figures S21-S26, Table 2). The anodic-to-cathodic peak potential separation (ΔE) was also determined for each event across the range of scan rates, and subsequently used in conjunction with the diffusion coefficient to calculate the heterogeneous electron-transfer rate constants for each redox event, per the Nicholson method (Figures S21-S26). These values are summarized in Table 2.

In our previous work with homoleptic POV-alkoxide clusters, $[V_6O_7(OR)_{12}]$ (R = CH_3, C_2H_5, C_3H_7, C_4H_9), we observed that increasing alkoxide chain length results in no change to the diffusion or electron-transfer kinetics of the redox events. Similarly, here we observe that extension to bridging-pentoxides in **1-pentyl** has minimal effect on the electrochemical properties of the system. Yet a further increase in carbon chain length, as in the case of **1-hexyl**, results in significant loss of redox activity, evidenced by the complete loss of reversibility in the four observed redox events for the compound. In fact, the diffusion kinetics for **1-hexyl** are so diminished that CV experiments at fast scan rates (>500 mV/s) yield no current response (Figure S27). As a result of the sluggish diffusion kinetics, the D_0 and k_0 values for **1-hexyl** cannot be calculated. The diminished electrochemical profile of **1**-hexyl marks the only example of synthetic modification we have made at the surface of the POV-alkoxide clusters which alters the electrochemical properties of the hexavanadium core. This result indicates that although the platform is modular, there are limitations to ligand modifications that can be tolerated.

In assessing the electrochemical performance of the mixed POV-alkoxides, the D_0 and k_0 values for each of the redox events in **2-ethyl**, **2-propyl**, **2-butyl**, and **2-pentyl** are comparable to those determined for the homoleptic clusters (Table). In measuring the CV of **2-hexyl**, we note that, unlike its homoleptic analogue **1-hexyl**, a linearly increasing current response can be observed with increasing scan rate for three of the four redox events (Figure S26). The exception is the most reducing event ($E_{1/2}$ = −0.79 V), which is irreversible at scan rates >500 mV/s. The redox properties of **2-hexyl** mark significant improvement

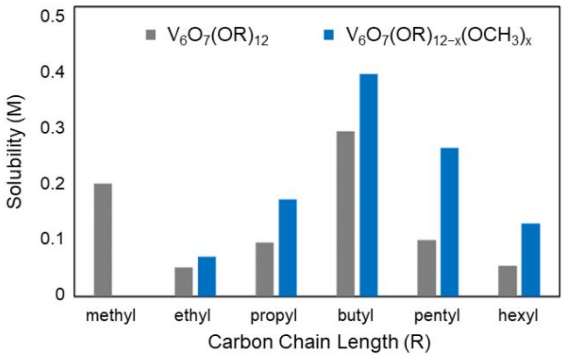

Figure 5. Solubility of each species measured in acetonitrile with 0.1 M $[NBu_4][BH_4]$ to mimic NRFB cell conditions.

over the electrochemical profile **1-hexyl**, again illustrating the ability of partial incorporation of shorter-chain alkoxide ligands to mitigate the deleterious electrochemical effects of long-chain alkoxide ligands at the surface of polyoxovanadate clusters.

Understanding the physical properties that affect the diffusion and electron-transfer rates of a charge carrier is fundamentally important, as these are critical limiting factors in the voltage efficiency of RFB devices. In mononuclear metal-based charge carriers, it has been previously demonstrated that delocalization yields rapid electron-transfer for a variety of metal centres, as in the case of metallocene complexes.[55] Multinuclear aqueous POM-based charge carriers have demonstrated similarly rapid kinetics, with $k_0 \approx 10^{-2}$ for both redox events in $[SiW_{12}O_{40}]^{4-}$, remarkably fast for electron-transfer in water.[43] Our previous work has established that the delocalized electronic structure of the POV-alkoxide platform is capable of facilitating rapid charge transfer, even with fairly extensive homoleptic and site-selective ligand modifications.[47, 50] Here, we establish limitations to the extent that surface modifications to the POV-alkoxide platform can be made without affecting electrochemical performance. However, this investigation of classically "impure" heteroleptic cluster establishes new routes to offset the observed electrochemical consequences of integrating long-chain alkoxide ligands.

Charge-discharge cycling of POV-alkoxides

To assess the redox stability of the POV-alkoxide clusters under the chemical conditions of a RFB cell, we used bulk electrolysis in conjunction with CV monitoring of solutions in their fully charged and fully discharged states. We have used similar experiments previously to demonstrate the electrochemical stability of $[V_6O_7(OR)_{12}]$.[45,50] Here, we found that bulk oxidation and reduction to 1.0 V and −1.0 V, respectively, yields no change in the redox profiles of **1-pentyl**, **2-ethyl**, **2-propyl**, **2-butyl**, and **2-pentyl**, apart from the expected shifts in open circuit potential (Figures S28-S32). The accessibility and stability of the fully charged derivatives of these clusters suggests that they are capable of functioning as two-electron charge carriers in *symmetric* NRFB schematics. In contrast, the analogous bulk electrolysis experiments for **1-hexyl** and **2-hexyl**, resulted in decomposition of the cluster core, as confirmed *via* CV (Figures S33-S34).

To more rigorously assess whether the presence of "mixed" bridging-alkoxide ligands impacts the electrochemical performance of these molecules, we conducted a series of charge-discharge experiments using both the homoleptic and mixed clusters. While the focus of this discussion will be to compare the performance of **1-pentyl** and **2-pentyl**, results of analogous experiments comparing **1-propyl** vs. **2-propyl** and **1-butyl** vs. **2-butyl** are detailed in the supporting information (Figures S35-S36). The charge-discharge experiments of complexes **1-hexyl** and **2-hexyl** were not performed given the electrochemical instability of these molecules (*vide supra*). The CVs of **1-pentyl** and **2-pentyl** suggest that each can be used to construct a symmetric NRFB cell wherein the cluster serves as both the anolyte and catholyte, cycling two electrons at each electrode. To test their capabilities in such a charging schematic, identical solutions of each neutral compound were prepared and used to fill both halves of a two-compartment H-cell divided by a microporous frit (1.6 µm). Each half of the H-cell contained 5 mL of solution, with 2 mM concentration of the active species (either **1-pentyl** or **2-pentyl**), along with 0.1 M $[NBu_4][PF_6]$ supporting electrolyte in acetonitrile. Carbon mesh electrodes (1 cm^3) were submerged in each compartment of the cell, and galvanostatic cycling was performed to 70 % state of charge (SOC). Charging and discharging currents were set to 0.4

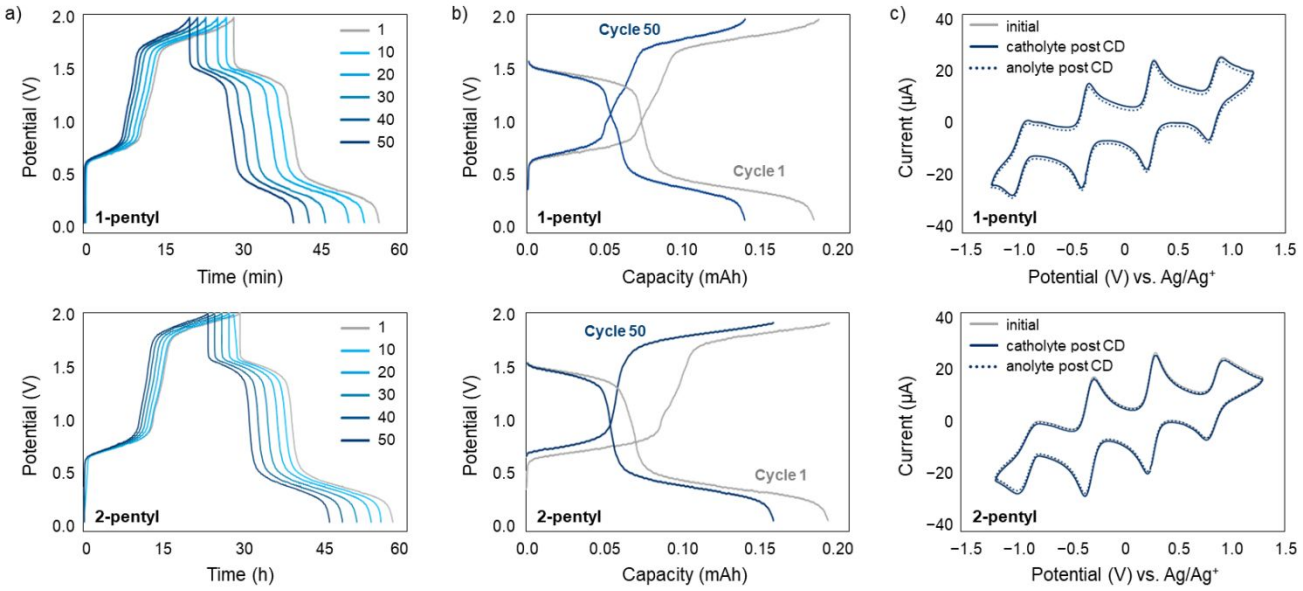

Figure 6. (a) Voltage trace of charge discharge experiments with 1-pentyl (top) and 2-pentyl (bottom). (b) Capacity vs. Potential for cycles 1 and 50 of charge discharge experiments with 1-pentyl (top) and 2-pentyl (bottom). (c) Cyclic voltammograms of anolyte and catholyte solutions of 1-pentyl (top) and 2-pentyl (bottom) before and after charge discharge experiments.

mA, with potential cut-offs of 2.0 V charging and 0.1 V discharging to enable cycling through the desired two-electron transformations at each electrode.

Charge-discharge cycling of complexes **1-pentyl** and **2-pentyl** was conducted for 50 cycles for a total of ~60 hours. In the voltage trace of the charge-discharge experiments for both homo- and heteroleptic POV-alkoxide clusters, two distinct charging plateaus are observed, the first at 0.7 V and the second at 1.7 V, falling to 1.4 V and 0.4 V upon discharge of the cell (Figure 6a). The potentials of each charging plateau are in good agreement with the expected potentials based on CV experiments, and are indicative of two separate, one-electron redox events. Likewise two distinct one electron discharging events are observed, with discharge-plateaus at lower potentials—typical in H-cell charging schematics.[45-47, 56] For **1-pentyl,** the initial SOC was 0.18 mAh (67 %), falling to 0.14 mAh (52 %) by cycle 50, while for **2-pentyl**, the initial SOC was 0.19 mAh (71 %), falling to 0.16 mAh (60 %) (Figure 6b). While there is a slight reduction in capacity fade for **2-pentyl** compared to **1-pentyl**, we are hesitant to attribute this to improved physicochemical properties of the mixed POV-alkoxide, owing to the small magnitude of the observed change. The coulombic efficiency for both **1-pentyl** and **2-pentyl** remained >97 % throughout charge-discharge cycling (Figure S37), highlighting the stable electron transfer to and from these POV-alkoxide clusters.

Charge carrier stability during battery cycling is critical for RFB application, as it is the major determining factor of device efficiency and lifetime. In order to rigorously assess the stability of the **1-pentyl** and **2-pentyl** during charge-discharge, we examined CVs of the anolyte and catholyte solutions following each cycling experiment (Figure 6c). Analysis reveals no shifts in the $E_{1/2}$ of each redox event or significant losses in current response, confirming that both homo- and heteroleptic POV-alkoxide clusters do not degrade during charge cycling experiments.

Conclusion

Synthetic chemistry is largely focused on the discovery and isolation of analytically pure compounds. More and more, however, we are beginning to understand the critical role that the presence of classically defined "impurities" play in promoting desired molecular activity. For example, in medicinal chemistry, attempts to synthesize natural product mimics of botanical remedies often yield isolated compounds which have reduced antimicrobial activity, while mixtures are favoured for eliciting the desired function.[57] Such synergistic effects are not restricted to biological applications; multimetallic nanostructures have been frequently been cited for improved catalytic activity due to the presence of the "impure" second metal.[58-61] In materials chemistry, it is well established that the introduction of impurities *via* doping to create surface defects can yield significantly improved properties in bulk systems, with prominent applications in energy storage, catalysis, and photocatalysis.[62-66] These examples highlight the ability for "defects" (or impurities) at the molecular level to introduce wholly new reactivities for the bulk system.

In the context of RFBs, it has been reported that the use of mixed-acid electrolyte solution improves solubility and stability of aqueous all-vanadium systems over those using pure sulfuric acid.[67] The effects of vanadium source impurities and additives have also been explored, in an effort to improve the thermal stability of the charge carrier in solution.[68] To date, however, the role of impurities in molecular charge carriers has not been studied. Indeed, the major focus of charge carrier discovery in recent years has been to synthetically target and isolate "designer" redox active molecules in order to elicit improved charge carrier function. This includes our recent work functionalizing POV-alkoxides with ether-based TRIOL ligands for the purpose of increasing system solubility.[47] These studies are certainly important for understanding how specific structural modifications affect the overall physicochemical properties of a molecule. However, the potential for improved properties to result from a mixture of charge carriers highlights the molecular synergy possible when similar complexes are blended for electrochemical energy storage.

Here, we report our results concerning the potential implications of using classically impure molecular mixtures as charge carriers for NRFB applications. Although the homoleptic POV-methoxide cluster, $[V_6O_7(OCH_3)_{12}]$, is electrochemically unstable upon oxidation, the introduction of methoxide "impurities" to longer-chain POV-alkoxides can improve both the physical and electrochemical properties of these systems beyond either "pure" derivative. For application in grid-scale energy storage, the improved properties in these "mixed" solutions are particularly intriguing, as the absence of extensive purification processes has positive implications for simplified scaling and cost reduction. These results suggest an additional avenue of exploration in the development of new charge carriers for solution-state energy storage.

Conflicts of interest

There are no conflicts to declare.

Acknowledgements

The authors gratefully acknowledge Anjula M. Kosswattaarachchi and Prof. Timothy R. Cook for helpful discussions and surrounding electrochemical analysis of polyoxovanadium-alkoxide charge carriers. The authors would like to thank the University of Rochester for funding supporting this research, and the National Science Foundation (MRI-1725028). L. E. V. is supported by the National Science Foundation Graduate Research Fellowship Program (DGE-1419118).

Notes and references

1 M. J. I. Gyuk, J. Vetrano, K. Lynn, W. Parks, R. Hnada, L. Kannberg, S. Hearne, K. Waldrip, R. Braccio, *Journal*, 2013.

2 W. A. Braff, J. M. Mueller and J. E. Trancik, *Nature Climate Change*, 2016, **6**, 964.
3 Z. Yang, J. Zhang, M. C. W. Kintner-Meyer, X. Lu, D. Choi, J. P. Lemmon and J. Liu, *Chemical Reviews*, 2011, **111**, 3577-3613.
4 B. Dunn, H. Kamath and J.-M. Tarascon, *Science*, 2011, **334**, 928-935.
5 J. Cho, S. Jeong and Y. Kim, *Progress in Energy and Combustion Science*, 2015, **48**, 84-101.
6 G. L. Soloveichik, *Annual Review of Chemical and Biomolecular Engineering*, 2011, **2**, 503-527.
7 T. M. Gür, *Energy & Environmental Science*, 2018, **11**, 2696-2767.
8 A. Z. Weber, M. M. Mench, J. P. Meyers, P. N. Ross, J. T. Gostick and Q. Liu, *Journal of Applied Electrochemistry*, 2011, **41**, 1137.
9 P. Leung, X. Li, C. Ponce de León, L. Berlouis, C. T. J. Low and F. C. Walsh, *RSC Advances*, 2012, **2**, 10125-10156.
10 W. Wang, Q. Luo, B. Li, X. Wei, L. Li and Z. Yang, *Advanced Functional Materials*, 2013, **23**, 970-986.
11 G. L. Soloveichik, *Chemical Reviews*, 2015, **115**, 11533-11558.
12 R. M. Darling, K. G. Gallagher, J. A. Kowalski, S. Ha and F. R. Brushett, *Energy & Environmental Science*, 2014, **7**, 3459-3477.
13 K. Gong, Q. Fang, S. Gu, S. F. Y. Li and Y. Yan, *Energy & Environmental Science*, 2015, **8**, 3515-3530.
14 M. H. Chakrabarti, R. A. W. Dryfe and E. P. L. Roberts, *Electrochimica Acta*, 2007, **52**, 2189-2195.
15 D. Zhang, H. Lan and Y. Li, *Journal of Power Sources*, 2012, **217**, 199-203.
16 C. G. Armstrong and K. E. Toghill, *Journal of Power Sources*, 2017, **349**, 121-129.
17 K. H. Hendriks, S. G. Robinson, M. N. Braten, C. S. Sevov, B. A. Helms, M. S. Sigman, S. D. Minteer and M. S. Sanford, *ACS Central Science*, 2018, **4**, 189-196.
18 A. M. Kosswattaarachchi, A. E. Friedman and T. R. Cook, *ChemSusChem*, 2016, **9**, 3317-3323.
19 J. Winsberg, C. Stolze, S. Muench, F. Liedl, M. D. Hager and U. S. Schubert, *ACS Energy Letters*, 2016, **1**, 976-980.
20 X. Wei, W. Xu, J. Huang, L. Zhang, E. Walter, C. Lawrence, M. Vijayakumar, W. A. Henderson, T. Liu, L. Cosimbescu, B. Li, V. Sprenkle and W. Wang, *Angewandte Chemie International Edition*, 2015, **54**, 8684-8687.
21 A. P. Kaur, N. E. Holubowitch, S. Ergun, C. F. Elliott and S. A. Odom, *Energy Technology*, 2015, **3**, 476-480.
22 J. Winsberg, T. Hagemann, S. Muench, C. Friebe, B. Häupler, T. Janoschka, S. Morgenstern, M. D. Hager and U. S. Schubert, *Chemistry of Materials*, 2016, **28**, 3401-3405.
23 Y. Huang, S. Gu, Y. Yan and S. F. Y. Li, *Current Opinion in Chemical Engineering*, 2015, **8**, 105-113.
24 J. A. Kowalski, L. Su, J. D. Milshtein and F. R. Brushett, *Current Opinion in Chemical Engineering*, 2016, **13**, 45-52.
25 S.-H. Shin, S.-H. Yun and S.-H. Moon, *RSC Advances*, 2013, **3**, 9095-9116.
26 R. Dmello, J. D. Milshtein, F. R. Brushett and K. C. Smith, *Journal of Power Sources*, 2016, **330**, 261-272.
27 J. Winsberg, T. Hagemann, T. Janoschka, M. D. Hager and U. S. Schubert, *Angewandte Chemie International Edition*, 2017, **56**, 686-711.
28 P. J. Cappillino, H. D. Pratt, N. S. Hudak, N. C. Tomson, T. M. Anderson and M. R. Anstey, *Advanced Energy Materials*, 2014, **4**, 1300566.
29 P. J. Cabrera, X. Yang, J. A. Suttil, R. E. M. Brooner, L. T. Thompson and M. S. Sanford, *Inorganic Chemistry*, 2015, **54**, 10214-10223.
30 J. A. Suttil, J. F. Kucharyson, I. L. Escalante-Garcia, P. J. Cabrera, B. R. James, R. F. Savinell, M. S. Sanford and L. T. Thompson, *Journal of Materials Chemistry A*, 2015, **3**, 7929-7938.
31 H. Wang, S. Hamanaka, Y. Nishimoto, S. Irle, T. Yokoyama, H. Yoshikawa and K. Awaga, *Journal of the American Chemical Society*, 2012, **134**, 4918-4924.
32 Y. Nishimoto, D. Yokogawa, H. Yoshikawa, K. Awaga and S. Irle, *Journal of the American Chemical Society*, 2014, **136**, 9042-9052.
33 M. Genovese and K. Lian, *Current Opinion in Solid State and Materials Science*, 2015, **19**, 126-137.
34 H. Yoshikawa, C. Kazama, K. Awaga, M. Satoh and J. Wada, *Chemical Communications*, 2007, DOI: 10.1039/B707189B, 3169-3170.
35 M. Pope, *Heteropoly and Isopoly Oxometalates*, Springer-Verlag Berlin Heidelberg, 1983.
36 A. M. M Pope, *Polyoxometalate Chemistry: From Topology via Self-Assembly to Applications*, Springer, Netherlands, 2001.
37 L. Cronin and A. Muller, *Chemical Society Reviews*, 2012, **41**, 7333-7334.
38 D.-L. Long, E. Burkholder and L. Cronin, *Chemical Society Reviews*, 2007, **36**, 105-121.
39 H. D. Pratt, N. S. Hudak, X. Fang and T. M. Anderson, *Journal of Power Sources*, 2013, **236**, 259-264.
40 H. D. Pratt Iii and T. M. Anderson, *Dalton Transactions*, 2013, **42**, 15650-15655.
41 H. D. Pratt, W. R. Pratt, X. Fang, N. S. Hudak and T. M. Anderson, *Electrochimica Acta*, 2014, **138**, 210-214.
42 J.-J. Chen, M. D. Symes and L. Cronin, *Nature Chemistry*, 2018, **10**, 1042-1047.
43 J. Friedl, M. V. Holland-Cunz, F. Cording, F. L. Pfanschilling, C. Wills, W. McFarlane, B. Schricker, R. Fleck, H. Wolfschmidt and U. Stimming, *Energy & Environmental Science*, 2018, **11**, 310-3018.
44 J.-J. J. Chen and M. A. Barteau, *Journal of Energy Storage*, 2017, **13**, 255-261.
45 L. E. VanGelder, A. M. Kosswattaarachchi, P. L. Forrestel, T. R. Cook and E. M. Matson, *Chemical Science*, 2018, **9**, 1692-1699.
46 L. E. VanGelder and Ellen M. Matson, *Journal of Materials Chemistry A*, 2018, **6**, 13874-13882.
47 L. E. VanGelder, B. E. Petel, O. Nachtigall, G. Martinez, W. W. Brennessel and E. M. Matson, *ChemSusChem*, **0**.
48 C. Daniel and H. Hartl, *Journal of the American Chemical Society*, 2005, **127**, 13978-13987.
49 O. Nachtigall and J. Spandl, *Chemistry – A European Journal*, 2018, **24**, 2785-2789.
50 A. M. Kosswattaarachchi, L. E. VanGelder, O. Nachtigall, J. P. Hazelnis, W. W. Brennessel, E. M. Matson, and T. R. Cook, *Submitted*.
51 J. Spandl, C. Daniel, I. Brüdgam and H. Hartl, *Angewandte Chemie International Edition*, 2003, **42**, 1163-1166.
52 J. Spandl, C. Daniel, I. Brudgam and H. Hartl, *Angew. Chem., Int. Ed.*, 2003, **42**, 1163-1166.
53 C. S. Sevov, S. L. Fisher, L. T. Thompson and M. S. Sanford, *Journal of the American Chemical Society*, 2016, **138**, 15378-15384.
54 C. Daniel and H. Hartl, *Journal of the American Chemical Society*, 2009, **131**, 5101-5114.
55 Y. Ding, Y. Zhao, Y. Li, J. B. Goodenough and G. Yu, *Energy & Environmental Science*, 2017, **10**, 491-497.
56 A. M. Kosswattaarachchi and T. R. Cook, *Electrochimica Acta*, 2018, **261**, 296-306.
57 D. J. Newman and G. M. Cragg, *Journal of Natural Products*, 2012, **75**, 311-335.
58 C. P. Vinod, A. B. Vysakh and S. Sreedhala, in *Metal Nanoparticles and Clusters: Advances in Synthesis, Properties and Applications*, ed. F. L. Deepak, Springer International Publishing, Cham, 2018, DOI: 10.1007/978-3-319-68053-8_5, pp. 165-199.
59 H. Lan, X. Xiao, S. Yuan, B. Zhang, G. Zhou and Y. Jiang, *Catalysis Letters*, 2017, **147**, 2187-2199.

60 Y. Hong, H. Zhang, J. Sun, K. M. Ayman, A. J. R. Hensley, M. Gu, M. H. Engelhard, J.-S. McEwen and Y. Wang, *ACS Catalysis*, 2014, **4**, 3335-3345.
61 A. K. Singh and Q. Xu, *ChemCatChem*, 2013, **5**, 652-676.
62 G. A. Somorjai, K. M. Bratlie, M. O. Montano and J. Y. Park, *The Journal of Physical Chemistry B*, 2006, **110**, 20014-20022.
63 X. Zhang, J. Qin, Y. Xue, P. Yu, B. Zhang, L. Wang and R. Liu, *Scientific Reports*, 2014, **4**, 4596.
64 M. Behrens, F. Studt, I. Kasatkin, S. Kühl, M. Hävecker, F. Abild-Pedersen, S. Zander, F. Girgsdies, P. Kurr, B.-L. Kniep, M. Tovar, R. W. Fischer, J. K. Nørskov and R. Schlögl, *Science*, 2012, **336**, 893-897.
65 P. Simon and Y. Gogotsi, *Accounts of Chemical Research*, 2013, **46**, 1094-1103.
66 Z. Yang, J. Ren, Z. Zhang, X. Chen, G. Guan, L. Qiu, Y. Zhang and H. Peng, *Chemical Reviews*, 2015, **115**, 5159-5223.
67 D. Reed, E. Thomsen, B. Li, W. Wang, Z. Nie, B. Koeppel, J. Kizewski and V. Sprenkle, *Journal of The Electrochemical Society*, 2016, **163**, A5211-A5219.
68 L. Cao, M. Skyllas-Kazacos, C. Menictas and J. Noack, *Journal of Energy Chemistry*, 2018, **27**, 1269-1291.